Origin of large positive magnetoresistance in the hard-gap regime of epitaxial Co-doped ZnO ferromagnetic semiconductors

Y. F. Tian,[1,2] Shi-shen Yan,[1,*] Q. Cao,[1] J. X. Deng,[1] Y. X. Chen,[1] G. L. Liu,[1] L. M. Mei,[1] and Y. Qiang[2,†]
[1]*School of Physics and National Key Laboratory of Crystal Materials, Shandong University, Jinan, Shandong 250100, People's Republic of China*
[2]*Department of Physics, University of Idaho, Moscow, Idaho 83844, USA*
(Received 15 October 2008; revised manuscript received 26 December 2008; published 20 March 2009)

We studied the electrical transport properties of single-crystal epitaxial Co-doped ZnO films grown by molecular-beam epitaxy. Upon increasing temperature, transport mechanisms changed from hard-gap resistance to Efros variable range hopping. The magnetic field and the temperature dependence of magnetoresistance revealed that large positive magnetoresistance observed in the hard-gap regime originated from the shrinkage of electron wave functions. However, no sign of spin-dependent transport behavior was found.

DOI: 10.1103/PhysRevB.79.115209 PACS number(s): 72.20.Ee, 72.80.Ey, 73.61.Ga, 72.25.Dc

Transition-metal (TM)-doped wide band-gap oxide semiconductors are of great interest as spintronics materials since the prediction of high Curie temperature in TM-doped ZnO.[1] It is commonly believed that the intrinsic ferromagnetism of the TM-doped oxide magnetic semiconductors results from the s,p-d hybridization interactions between the conducting or weakly localized s,p carriers and the strongly localized $3d$ electrons of the doped TM elements. Therefore, TM-doped oxide magnetic semiconductors are expected to supply not only intrinsic high-temperature ferromagnetism but also spin-polarized carriers. However, the intrinsic ferromagnetism is still in debate[2–4] because intensive studies on magnetism and microstructures are contradictory. On the other hand, spin-dependent electrical transport of TM-doped oxide magnetic semiconductors is less known, especially the mechanism of electrical transport and the origin of magnetoresistance (MR),[5–9] which may throw new light on the origin of ferromagnetism. Some researchers believe that the positive magnetoresistance (PMR) obtained in Co-doped ZnO, Mn-doped ZnO, and Co-doped TiO_2 can be attributed to the spin splitting effect of the conduction band due to strong s-d exchange interaction between carriers and doped TM atoms,[5–7] while other researchers believe that PMR in Co-doped ZnO results from the action of Lorentz force on the mobile carriers.[8,9] Moreover, similar PMR phenomena observed in GaAs, $CuInSe_2$, and $CuGaSe_2$ are attributed to the shrinkage of carrier's wave function in an applied magnetic field.[10–12] Understanding the different origins of PMR and quantitative studies on the electrical transport properties of TM-doped oxide magnetic semiconductors are necessary not only for solving current theoretical issues but also for designing future spintronics devices.

In this paper, we report that the electrical transport properties of Co-doped ZnO single-crystal magnetic semiconductor films can be well explained by combining the Efros variable range hopping (VRH) and the hard-gap resistance. The magnetic field and temperature dependence of the PMR indicate that the observed PMR in the hard-gap regime comes from carrier's wave-function shrinkage under an applied magnetic field.

Since high-quality single-crystal ZnO-based films are ideal samples for understanding the intrinsic properties of oxide diluted magnetic semiconductor (DMS), single-crystal $Zn_{1-x}Co_xO$ (x is the atomic concentration of the doping cobalt) films of 600 nm in thickness were grown by radiofrequency oxygen plasma-assisted molecular-beam epitaxy on commercial Al_2O_3 (0001) substrates. Microstructures were measured by *in situ* reflection high-energy electron diffraction and *ex situ* high-resolution x-ray diffraction, revealing that single-crystal Co-doped ZnO with wurtzite structure was obtained. Shakeup satellites of Co $2p_{1/2}$ and $2p_{3/2}$ photoelectron peaks were observed by *in situ* x-ray photoelectron spectroscopy measurements, revealing that Co cations were in the +2 oxidation state, which was consistent with Co substitution. Magnetic properties were measured by superconducting quantum interference device (SQUID) in the temperature range from 5 to 300 K. Ferromagnetism was obtained up to room temperature. However, the average moment of Co at room temperature is relatively small. For example, the saturation moment is $\sim 0.14\mu_B$/Co at 300 K for $x=0.021$ as shown in Fig. 2(b) if all Co atoms are assumed to contribute equally to the moment. It increases to $\sim 2.4\mu_B$/Co at 5 K. Detailed preparation conditions, microstructures, and magnetic results of samples with different Co doping concentration have been published elsewhere.[4] The electrical transport properties were measured in the Van der Pauw configuration by SQUID using Keithley 2400 as current source and Keithley 2182 as voltage detector. Applied magnetic field was parallel to both the film plane and current flow. Isothermal MR is defined as $\mathrm{MR}=[\rho(H,T)-\rho(0,T)]/\rho(0,T)\times 100\%$. Here, $\rho(H,T)$ is the sample sheet resistance in an applied magnetic field H.

Figure 1 shows the temperature dependence of the sheet resistance with 0 and 5 T magnetic field. In Fig. 1(a), a linear relationship between $\ln\rho$ and T^{-1} was observed in the low-temperature range for zero-field resistance. This reveals the existence of a hard gap in the density of states near the Fermi level.[13–15] On the other hand, notice that $\ln\rho$ deviated from this linear relationship under a 5 T magnetic field, and a large increasing of sheet resistance (large PMR) in the hard-gap regime was observed. This indicates that the magnetic field changes the electrical transport mechanisms.

There are two kinds origin of hard gap: magnetic origin which is due to the exchange interaction between itinerant

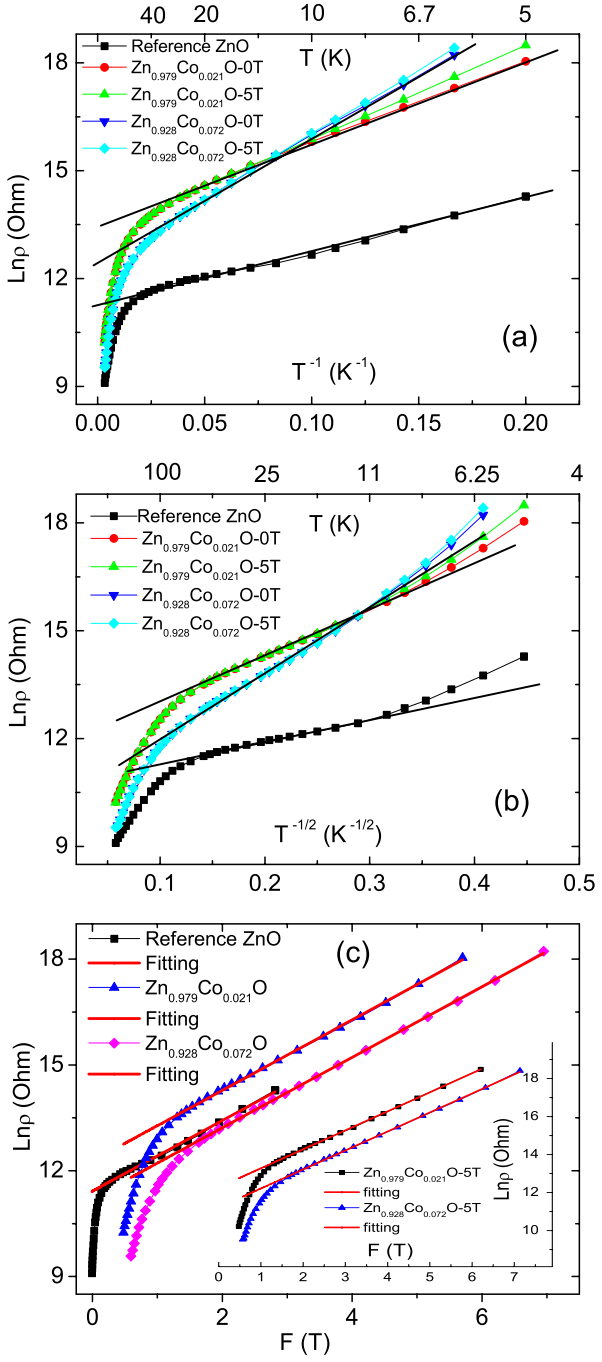

FIG. 1. (Color online) The temperature dependence of ln ρ vs (a) T^{-1}, (b) $T^{-1/2}$, and (c) $F(T)=\{(T_{ES}/T)^{1/2}+E_H/k_BT\}$ for $Zn_{0.979}Co_{0.021}O$, $Zn_{0.928}Co_{0.072}O$, and reference ZnO samples with and without magnetic field. Actual temperature is given on the top axes for Figs. 1(a) and 1(b). The inset theoretical fittings in Fig. 1(c) include contributions from both Eqs. (1) and (3), which can well describe the resistance in a 5 T magnetic field.

carriers and localized TM atoms[13] and nonmagnetic origin which is due to electron polaron excitations caused by multielectron interaction effects.[14,15] It should be pointed out that those short-range many-electron excitation effects in the nonmagnetic origin are caused by long-range single electron hopping;[15] hence, pure hard-gap transport cannot exist without Efros variable range hopping which will be mentioned below. Since the nonmagnetic reference ZnO sample shows the same linear relationship between ln ρ and T^{-1} at low temperature, the hard gap is supposed to have a nonmagnetic origin.

When the temperature is out of the hard-gap transport regime, the sheet resistance becomes almost the same with and without applied magnetic field, i.e., MR disappears. In this temperature range a linear relationship between ln ρ and $T^{-1/2}$ is observed as given in Fig. 1(b). This behavior is typical of Efros VRH (Ref. 16) due to the long-range Coulomb interactions between carriers. Obvious deviation from this linear relationship is observed at high temperature. This is because thermal activation at high temperature allows other transport paths and the electrical transport becomes rather complicated which is far beyond our current discussion.

The crossover from the hard-gap resistance to Efros VRH with increasing temperature is clearly seen in Figs. 1(a) and 1(b). Because energy is additive,[17,18] the sheet resistance at zero magnetic field should be well described by considering the contribution from both the Coulomb interaction and the hard-gap energy, i.e.,

$$\rho = \rho_0 \exp\{(T_{ES}/T)^{1/2} + E_H/k_BT\}. \quad (1)$$

Here, ρ_0 is a resistance prefactor, T_{ES} is the characteristic temperature for Efros VRH, E_H is the hard-gap energy, and k_B is the Boltzmann constant. Detailed discussions can be found in our previous work.[18] Figure 1(c) shows theoretical fittings to the zero-field experimental resistance according to Eq. (1). It is clear that ln ρ linearly depends on $F(T)=\{(T_{ES}/T)^{1/2}+E_H/k_BT\}$ in a wider temperature range with fitting parameters for $Zn_{0.979}Co_{0.021}O$ (T_{ES}=57.968 K, E_H/k_B=11.491 K, and ρ_0=214 747 Ω) and for $Zn_{0.928}Co_{0.072}O$ (T_{ES}=75.796 K, E_H/k_B=20.376 K, and ρ_0=74 339 Ω). Using a reasonable dielectric constant $\kappa=10\varepsilon_0$(ε_0 is the vacuum dielectric constant) for bulk ZnO according to Ref. 19, we can derive that the localization length $\xi=8e^2/\kappa k_BT_{ES}$ at 5 K is 230 nm for $Zn_{0.979}Co_{0.021}O$ and is 176 nm for $Zn_{0.928}Co_{0.072}O$. The optimal hopping distance $r=\xi(T_{ES}/T)^{1/2}/4$ at 5 K is 196 nm for $Zn_{0.979}Co_{0.021}O$ and is 171 nm for $Zn_{0.928}Co_{0.072}O$. From the doping concentration, we can calculate the average distance between dopant Co atoms, which is 1.05 nm for $Zn_{0.979}Co_{0.021}O$ and is 0.69 nm for $Zn_{0.9}Co_{0.072}O$. Therefore, the localization length and the optimal hopping distance of the carriers are in the same length scale at low temperature, which are much larger than the average distance between dopant Co atoms.

It is believed that an oxygen vacancy in Co-doped ZnO can trap one electron (s,p electron), which is weakly localized (has large localization length). Electrical transport is established via VRH of the weakly localized s,p carriers of oxygen vacancies. But the 3d electrons of Co atoms are strongly localized. Therefore, the carriers with large localization length can cover many Co atoms, which makes the Co atoms show ferromagnetic coupling due to the s,p-d exchange coupling between the weakly localized s,p electrons of the oxygen vacancies and the strongly localized d electrons of doped Co atoms. This is the so-called F-center model or bound magnetic polaron model of the ferromagnetism.[20,21] Our fitting parameters from the trans-

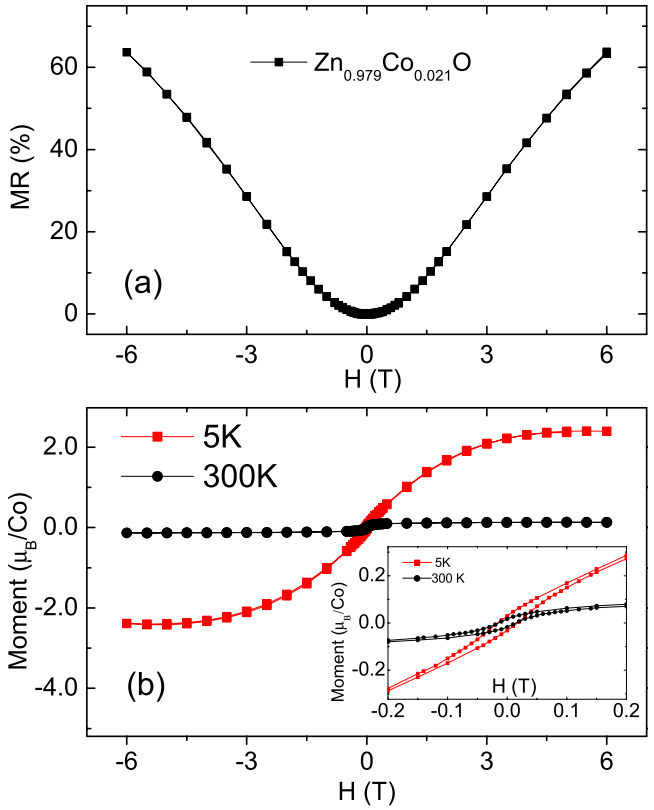

FIG. 2. (Color online) (a) The MR of $Zn_{0.979}Co_{0.021}O$ measured at 5 K. (b) SQUID hysteresis loops measured at 5 and 300 K for $Zn_{0.979}Co_{0.021}O$ thin film. The inset shows the zoom-in hysteresis loops.

port properties strongly support that the F-center or bound magnetic polaron model is the origination of ferromagnetism in our Co-doped ZnO DMSs.

Figure 2(a) shows a 64% PMR for $Zn_{0.979}Co_{0.021}O$ measured at 5 K. The reference ZnO only shows negligible PMR (<0.5% at 5 K) in the whole temperature range. A PMR in DMSs is usually ascribed to the giant spin splitting of band states caused by *s-d* exchange interaction.[5–7] In this case, PMR is found in a weak field, followed by a negative MR in higher magnetic field[5] or saturated in higher magnetic field,[22] which is different from our experimental results, i.e., nonsaturated PMR up to 6 T magnetic field. On the other hand, the hysteresis behavior in "butterfly" MR curves which are directly related to the spin-dependent hopping in ferromagnetic semiconductors with high Co concentration[23] is not observed here while the magnetization hysteresis loops are clearly observed as shown in Fig. 2(b). Also, it is clear that when the magnetic moment turns into saturation, the MR curve does not. This means that the MR curves are not directly related to the magnetization reversal.

Since a thick film of 600 nm can be recognized as a three-dimensional system rather than two dimensional, orbital effect can contribute to the electrical transport even though the applied magnetic field is parallel to the film plane. According to Ref. 16, the effect of a magnetic field on the wave function of carriers becomes stronger with increasing distance from the impurity center. Therefore, in the VRH conduction regime especially at sufficiently low temperatures where hopping distance is relatively large, one should expect a large PMR under applied magnetic field due to a sharp decrease in the overlap of wave-function "tails" between different states.

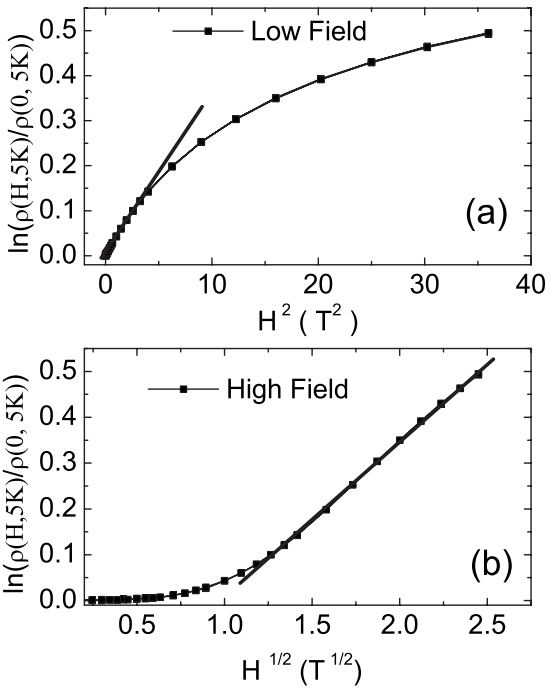

FIG. 3. The field dependence of $\ln(\rho(H,5K)/\rho(0,5K))$ as a function of (a) H^2 and (b) $H^{1/2}$ for $Zn_{0.979}Co_{0.021}O$ film. Solid straight lines are guides to the eyes.

At low magnetic field, the positive MR can be described by[14,16]

$$\ln\left(\frac{\rho(H,T)}{\rho(0,T)}\right) \propto \frac{\xi^4}{\lambda^4}\left(\frac{E_H}{k_B T}\right)^{3v}, \tag{2}$$

where $\lambda=(c\hbar/eH)^{1/2}$ is the characteristic magnetic length, ξ is the localization length of the carriers, and v is defined as the resistance exponent for the linear dependence of ln ρ on T^{-v} at zero field. Therefore, with $v=1$ in the hard-gap regime we get

$$\ln\left(\frac{\rho(H,T)}{\rho(0,T)}\right) \propto \frac{H^2}{T^3}. \tag{3}$$

This is consistent with the quadratic dependence on the magnetic field in a weak-field range as shown in Fig. 3(a).

At high magnetic field, the magnetic field localizes carriers in a much narrower region in the transverse direction than Coulomb potential does.[16] However, MR behavior in the hard-gap regime at strong magnetic field is less studied and is not well understood right now. As an approximation, we suppose that it can be described as $\ln(\rho(H,T)/\rho(0,T)) \propto f(H)/T^3$, similar to weak-field situation in temperature dependence. From Fig. 3(b) we obtain that $f(H)\sim H^{1/2}$ could well describe the MR behavior in the high magnetic field.

In Fig. 4, we plot $\ln(\rho(H,T)/\rho(0,T))$ as a function of T^{-n} with $H=5$ T. Good linear behavior is found for $Zn_{0.928}Co_{0.072}O$ with $n=3$. Moreover approximately linear behavior is found for $Zn_{0.979}Co_{0.021}O$ with $n=2.57$. This is

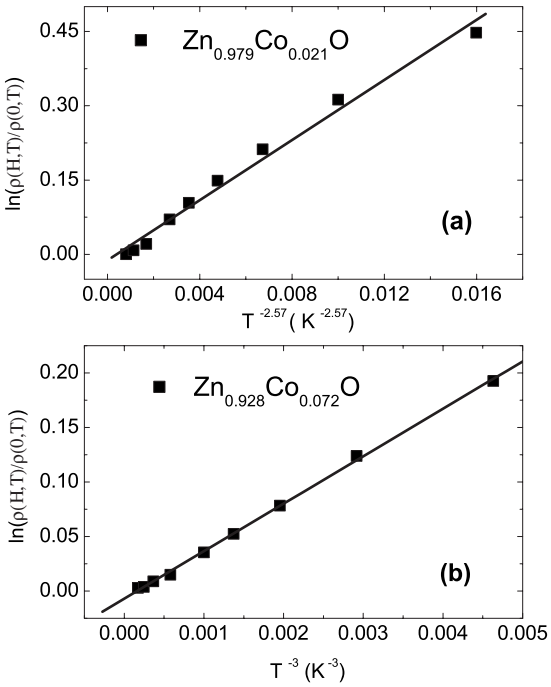

FIG. 4. $\ln(\rho(H,T)/\rho(0,T))$ as a function of T^{-n} for (a) $Zn_{0.979}Co_{0.021}O$ and (b) $Zn_{0.928}Co_{0.072}O$ at $H=5$ T. Solid straight lines are guides to the eyes.

consistent with the theoretical prediction $n=3$ in Eq. (3). Hence, the temperature dependence of MR further confirms that the observed large PMR results from the wave-function shrinkage of the carriers.

Finally, we discuss the role of Co doping played in our Co-doped ZnO single-crystal DMSs, and meanwhile we give an explanation of the absence of spin-dependent electrical transport. First of all, as mentioned above, Co doping provides localized 3*d* magnetic moments which participate into the formation of intrinsic ferromagnetism. Second, in principle, all electrical interactions and magnetic interactions take a role in the hopping process which can be regarded as electrical or magnetic energy barriers in Eq. (1), and the spin-dependent electrical transport properties only come from the magnetic interaction energies. However, as in our case the hopping distance is relatively large; the direct magnetic exchange energy between the initial and the final states can be ignored because they are short-range interactions. Other magnetic energies, such as Zeeman splitting energy and spin-orbit coupling energy, are much smaller than the electrical energies, such as Coulomb energy and hard-gap energy. As a result, no sign of spin-dependent transport behavior is macroscopically observed in spite of the large PMR in the low-temperature range. Third, from the original work of Ref. 16, we know that for the hopping transport in the weak-field regime, wave-function shrinkage related resistance variation can be expressed as $\rho(H,T)/\rho(0,T)=\exp((t\xi e^2H^2)/(Nc^2\hbar^2))$. Here, t is a constant, e is the electron charge, c is the velocity of light, $\hbar$ is the Planck constant, and N is the site concentration for the electrical transport. Fitting experimental results by Eq. (1), we obtained that the localization length ξ for the reference ZnO is 363 nm which is larger than that of Co-doped ZnO. Further, from our experiment results we know that large PMR is only observed in Co-doped ZnO though hard-gap transport is also observed in reference ZnO sample. This means that N should be much larger in the reference ZnO so that the ratio of ξ/N is much smaller in the reference ZnO film than in the Co-doped ZnO. In this sense, Co doping decreases the localization length ξ and greatly reduces the site concentration N, which leads to the observed large PMR. It should be noticed that the sheet resistance of Co-doped ZnO is much lager than that of reference ZnO prepared under the same condition. Considering that we used almost the same size samples for the transport measurements, larger sheet resistance is consistent with the decreasing localization length and site concentration in Co-doped ZnO DMSs.

In summary, the electrical transport properties of epitaxial single-crystal Co-doped ZnO ferromagnetic semiconductors with different Co doping concentrations were studied. It was found that hard-gap resistance changed to Efros VRH with increasing temperature. Temperature and magnetic field dependence of the observed large PMR confirmed that it was caused by carrier's wave-function shrinkage in a magnetic field, which was an orbital effect rather than spin effect of the carriers.

This work was supported by the State Key Project of Fundamental Research of China under Grants No. 2007CB924903 and No. 2009CB929202 and the NSF under Grants No. 50572053 and No. 10834001. In the University of Idaho, the research is partially supported by DOE-BES (Grant No. DE-FG02-07ER46386) and DOE-EPSCOR (Grant No. DE-FG02-04ER46142).

*shishenyan@sdu.edu.cn
†youqiang@uidaho.edu

[1] T. Dietl, H. Ohno, F. Matsukura, J. Cibert, and D. Ferrand, Science **287**, 1019 (2000).
[2] X. F. Wang, J. B. Xu, B. Zhang, H. G. Yu, J. Wang, X. X. Zhang, J. G. Yu, and Q. Li, Adv. Mater. (Weinheim, Ger.) **18**, 2476 (2006).
[3] T. Dietl, J. Appl. Phys. **103**, 07D111 (2008).
[4] G. L. Liu, Q. Cao, J. X. Deng, P. F. Xing, Y. F. Tian, Y. X. Chen, S. S. Yan, and L. M. Mei, Appl. Phys. Lett. **90**, 052504 (2007).
[5] Q. Xu, L. Hartmann, H. Schmidt, H. Hochmuth, M. Lorenz, R. S. Grund, C. Sturm, D. Spemann, and M. Grundmann, J. Appl. Phys. **101**, 063918 (2007).
[6] M. Sawicki, T. Dietl, J. Kossut, J. Igalson, T. Wojtowicz, and W. Plesiewicz, Phys. Rev. Lett. **56**, 508 (1986).
[7] S. R. Shinde, S. B. Ogale, S. Das Sarma, J. R. Simpson, H. D. Drew, S. E. Lofland, C. Lanci, J. P. Buban, N. D. Browning, V. N. Kulkarni, J. Higgins, R. P. Sharma, R. L. Greene, and

T. Venkatesan, Phys. Rev. B **67**, 115211 (2003).
[8] P. Stamenov, M. Venkatesan, L. S. Dorneles, D. Maude, and J. M. D. Coey, J. Appl. Phys. **99**, 08M124 (2006).
[9] L. Hartmann, Q. Xu, H. Schmidt, H. Hochmuth, M. Lorenz, C. Sturm, C. Meinecke, and M. Grundmann, J. Phys. D **39**, 4920 (2006).
[10] Q. Y. Ye, B. I. Shklovskii, A. Zrenner, F. Koch, and K. Ploog, Phys. Rev. B **41**, 8477 (1990).
[11] L. Essaleh, J. Galibert, S. M. Wasim, E. Hernández, and J. Leotin, Phys. Rev. B **52**, 7798 (1995).
[12] K. G. Lisunov, E. Arushanov, G. A. Thomas, E. Bucher, and J. H. Schön, J. Appl. Phys. **88**, 4128 (2000).
[13] P. Dai, Y. Zhang, and M. P. Sarachik, Phys. Rev. Lett. **69**, 1804 (1992).
[14] J. J. Kim and H. J. Lee, Phys. Rev. Lett. **70**, 2798 (1993).
[15] R. Chicon, M. Ortuño, and M. Pollak, Phys. Rev. B **37**, 10520 (1988).
[16] B. I. Shklovskii and A. L. Efros, *Electronic Properties of Doped Semiconductors* (Springer-Verlag, Berlin, 1984).
[17] A. Aharony, Y. Zhang, and M. P. Sarachik, Phys. Rev. Lett. **68**, 3900 (1992).
[18] Y. F. Tian, S. S. Yan, Y. P. Zhang, H. Q. Song, G. Ji, G. L. Liu, Y. X. Chen, and L. M. Mei, J. Appl. Phys. **100**, 103901 (2006).
[19] W. Tjhen, T. Tamagawa, C.-P. Ye, C.-C. Hsueh, P. Schiller, and D. L. Polla, IEEE Micro Electro Mechanical Systems, 1991, pp. 114-119.
[20] A. Kaminski and S. Das Sarma, Phys. Rev. Lett. **88**, 247202 (2002).
[21] J. M. D. Coey, M. Venkatesan, and C. B. Fitzgerald, Nature Mater. **4**, 173 (2005).
[22] H. H. Huang, C. A. Yang, P. H. Huang, C. H. Lai, T. S. Chin, H. E. Huang, H. Y. Bor, and R. T. Huang, J. Appl. Phys. **101**, 09H116 (2007).
[23] S. S. Yan, C. Ren, X. Wang, Y. Xin, Z. X. Zhou, L. M. Mei, M. J. Ren, Y. X. Chen, Y. H. Liu, and H. Garmestani, Appl. Phys. Lett. **84**, 2376 (2004).